LARGE-EDDY SIMULATION OF LIFTED TURBULENT METHANE/AIR DIFFUSION FLAMES

Heinz Pitsch*
Center for Turbulence Research
Stanford University
Stanford, CA
H.Pitsch@stanford.edu

Laurent Duchamp de Lageneste
Center for Turbulence Research
Stanford University
Stanford, CA
duchamp@ctr.stanford.edu

ABSTRACT

In recent years laminar flamelet models for turbulent non-premixed combustion have been successfully applied in Large-Eddy Simulations (LES). However, these models cannot describe premixed or partially premixed flame propagation, which is known to be of great importance in the stabilization region of lifted diffusion flames. In the present work a model proposed by Peters (2000) for Reynolds averaged models has been formulated for LES. Flamelet models for premixed and non-premixed combustion are combined to describe premixed, partially premixed, and non-premixed combustion. The G-equation model is used to describe premixed flame propagation. The turbulent burning velocity of the sub-grid scales appearing in this equation is evaluated as function of mixture fraction. The partially premixed post-flame region is described by a steady state laminar diffusion flamelet approach. The model is applied in numerical simulations of lifted methane/air diffusion flames. The predicted lift-off heights are in reasonable agreement with experimental data.

INTRODUCTION

Laminar flamelet models have successfully been used in numerical simulations of turbulent diffusion flames. Particularly attractive is the steady laminar flamelet model, which can be implemented very easily in numerical codes and requires no special treatment in the context of Large-Eddy Simulations (LES), leading to very good results in many situations. If unsteady effects are important the Lagrangian Flamelet Model has been shown to be capable of yielding very accurate predictions in Reynolds averaged (RANS) simulations (Pitsch et al. 1998, Pitsch 2000) and LES (Pitsch and Steiner 2000*a*, Pitsch and Steiner 2000*b*).

Although the Lagrangian Flamelet Model already adds some complexity to the calculations, it still has known deficiencies in predicting lifted flames and local extinction/reignition phenomena.

The physical process of the stabilization of diffusion flames away from the burner has been investigated for many years and several possible stabilization mechanisms have been suggested. Vanquickenborne and van Tiggelen (1966) for instance argued that at the stabilization point the fuel and oxidizer are perfectly premixed and in the mean the flow velocity equals the burning velocity at stoichiometric mixture. An alternative concept proposed by Peters and Williams (1983) explains flame liftoff by extinction of laminar flamelets. However, Pitts (1988) concludes in a review of these and other theories for the stabilization and blowout of jet diffusion flames that none of these theories is satisfactory.

More recent investigations suggest an important role of triple flame structures emphasizing the importance of the partially premixed nature of the liftoff problem (Kioni et al. 1993). Ruetsch et al. (1995) showed that the laminar flame speed of a triple flame is faster than the corresponding premixed flame, which is caused

*Author to whom correspondence should be send

by the divergence of the flow field ahead of the flame.

Based on these ideas Müller et al. (1994) formulated a model by combining a steady laminar diffusion flamelet model and the G-equation as a flamelet model for premixed combustion. In this model the turbulent burning velocity appearing in the G-equation is expressed based on the ideas of laminar triple flames and includes heat losses of the premixed flame front at stoichiometric conditions due to mixture fraction gradients and also the limit of flamelet quenching. The analysis shows that for the steady burning case the turbulent flame speed is strongly influenced by flamelet quenching.

Recently, Chen et al. (1999) presented a combined laminar diffusion flamelet/G-equation model. An important difference to the work of Müller et al. (1994) is that the influence of mixture fraction gradients on the laminar burning velocity is neglected. This is based on the experimental findings of Plessing et al. (1998) that in a laminar triple flame at a given mixture fraction the burning velocity is in good qualitative agreement with that of a perfectly premixed flame. Applied in RANS simulations the model shows very good agreement with experimental data.

In the present study a similar model will be formulated for LES. The G-equation will be used to describe the premixed front in the stabilization region and a laminar diffusion flamelet model for the post flame non-premixed combustion part. It has been discussed in earlier studies (Pitsch et al. 1998, Pitsch 2000) that the unsteadiness of the flamelet structure has to be considered if radiation is important or the formation of slowly developing pollutants is of interest. For the description of flame liftoff the application of a steady state flamelet model is expected to yield sufficient accuracy.

As a first validation step the model is applied in LES of lifted diffusion flames and compared to experimental data by (Muñiz and Mungal 1997).

NUMERICAL MODEL

In this section we will formulate a model similar to Peters (2000) and Chen et al. (1999) for LES. A laminar diffusion flamelet model will be used to describe the diffusion flame. Laminar flamelets are associated with a region in the vicinity of the surface of stoichiometric mixture and essentially describe the balance of chemical reactions with diffusive transport normal to iso-mixture fraction surfaces. The transport in this direction has been shown to be much more important than diffusive transport along the iso-mixture fraction surface. However, in lifted flames , in the stabilization region, transport along iso-surfaces of the mixture fraction is important. Hence, the laminar diffusion flamelet model has to be supplemented with a model that describes flame propagation in the stabilization region. Here, the G-equation will be used to distinguish between burning and non-burning regions.

The G-equation has been introduced by Williams (1985b) as

$$\frac{\partial G}{\partial t} + \boldsymbol{v} \cdot \nabla G = s_L |\nabla G|, \qquad (1)$$

where t is the time, $\boldsymbol{v}$ the velocity vector, and s_L is the laminar burning velocity. G is a non-reactive scalar describing the propagation of a premixed flame. The instantaneous location of the flame is given by an iso-scalar surface $G = G_0$, which divides the flow field into burnt and unburnt regions.

In the corrugated flamelet regime the laminar burning velocity s_L may be modified from that of an unstreched premixed flame by the influence of stretch. A modified expression for small curvature and strain has for instance been given by Pelce and Clavin (Pelce and Clavin 1982) as

$$s_L = s_L^0 - s_L^0 \mathcal{L}\kappa - \mathcal{L}S\,, \qquad (2)$$

where s_L^0 is the burning velocity of an unstreched premixed flame, κ is the curvature, S is the strain rate, and $\mathcal{L}$ is the Markstein length, which can be determined following for instance Clavin and Williams (1982) or Williams (1985a).

Since the laminar burning velocity s_L is a property of the flame, Eq. (1) is valid for $G = G_0$ only. Away from the front, the G-field has to be defined differently. A common approach is to use the constraint

$$|\nabla G| = 1, \qquad (3)$$

which makes the G-field a function describing the distance from the flame. Hence, the flame surface can be defined as being located at $G = 0$ and negative values of G correspond to unburnt, positive values of G to burnt gases.

Peters (1999) has derived an equation similar to Eq. (1) for the thin reaction zones regime and provided a combined equation, which is to

leading order valid for both regimes, as

$$\rho\frac{\partial G}{\partial t}+\rho\boldsymbol{v}\cdot\nabla G=\left(\rho s_L^0\right)|\nabla G|-(\rho D)\,\kappa|\nabla G|\,. \tag{4}$$

Equations for the Reynolds averaged mean and variance of G valid in both regimes have also been derived by Peters (1999). He also provided expressions for the turbulent burning velocity, which appears as the major unclosed term in the equations. In this derivation the time averaging is not trivial, since the instantaneous equation is only defined at $G = G_0$, and hence only information from this iso-surface can be used in the averaging. Peters (1999) presents a definition for mean and variance considering this requirement for a one-dimensional situation

An equation for the Favre-filtered value $\widetilde{G}$ can be obtained by similar arguments as in Peters (2000), yielding

$$\rho\frac{\partial\widetilde{G}}{\partial t}+\overline{\rho}\widetilde{\boldsymbol{v}}\cdot\nabla\widetilde{G}=(\overline{\rho}s_T^0)|\nabla\widetilde{G}|-\overline{\rho}D_t\widetilde{\kappa}|\nabla\widetilde{G}|, \tag{5}$$

where D_t is the sub-grid diffusivity and the turbulent burning velocity s_T^0 can be modeled by

$$\frac{s_T^0-s_L^0}{s_L^0}=-\frac{a_4b_3^2}{2b_1}\frac{\Delta}{l_F}+\left[\left(\frac{a_4b_3^2}{2b_1}\frac{\Delta}{l_F}\right)+a_4b_3^2\frac{v'\Delta}{s_L^0l_F}\right]^{1/2}. \tag{6}$$

Here, Δ is the filter size, l_F is the laminar flame thickness, and a_4, b_1, and b_3 are constants given in Peters (2000) for the Reynolds averaged model. The coefficient a_4 depends on the turbulent Schmidt number, for RANS assumed to be Sc_t=0.7. Following (Pitsch and Steiner 2000*a*) for LES the sub-grid Schmidt number can be approximated by Sc_t=0.4. Hence, a_4 can be re-evaluated for LES to be $a_4 = 1.37$. The other constants might differ for LES and have to be determined by DNS. Both the laminar burning velocity and the laminar flame thickness appearing in Eq. (6) are a function of the mixture fraction and are taken from unstreched laminar flame calculations.

It is clear from Eq. (6) that only the sub-grid contribution of the turbulent burning velocity is modeled and the major part, especially the flame front advancement from the large-scale velocity fluctuation, is resolved. It should be emphasized again that Eq. (5) is valid only for $\widetilde{G} = G_0$. The remaining $\widetilde{G}$-field is obtained by enforcing the condition given in Eq. (3) for $\widetilde{G}$ in a reinitialization procedure described in Russo and Smereka (2000).

In a recent study this model has been applied in an LES of a purely premixed turbulent flame and validated with experimental data (Duchamp de Lageneste and Pitsch 2000).

In order to solve the governing equations in an LES only the filtered density, and in the case of non-constant molecular properties also the temperature, is unknown and needs to be determined by a combustion model.

For the current model the filtered density is given as

$$\overline{\rho}^{-1}=\int_G\int_Z\rho^{-1}(Z,\chi_{\mathrm{st}},G)\widetilde{P}(Z)\widetilde{P}(G)dZdG\,. \tag{7}$$

Here, the probability density functions (pdfs) of Z, χ_{st}, and G are assumed to be independent. A β-function is used for the pdf of Z, a Gaussian function for the pdf of G, and a δ function has been assumed for the pdf of χ_{st}. The sub-grid variances of Z and G appearing in the presumed pdfs are determined using dynamic sub-grid scale models as described in Duchamp de Lageneste and Pitsch (2000). The density is given by

$$\rho\,(Z,\chi,G)=\begin{cases}\rho_1Z+\rho_2(1-Z), & \text{if } G<0\\ \rho(Z,\chi_{\mathrm{st}}) & \text{otherwise}\end{cases}, \tag{8}$$

where ρ_1 and ρ_2 are the densities of the fuel and the oxidizer stream, respectively, and $\rho(Z,\chi_{\mathrm{st}})$ is given by the solution of the steady flamelet equations.

Introducing Eq. (8) into Eq. (7) the mean density can be expressed as

$$\overline{\rho}^{-1}=\frac{1-p_b}{\rho_1\widetilde{Z}+\rho_2(1-\widetilde{Z})}+p_b\int_Z\rho^{-1}(Z,\chi_{\mathrm{st}})\widetilde{P}(Z)dZ \tag{9}$$

where p_b defined as

$$p_b=\int_{G_0}^{\infty}\widetilde{P}(G)dG \tag{10}$$

is the probability of finding burnt gases. Since the inverse of the unburnt density is only a weakly non-linear function, its convolution with the pdf of the mixture fraction has been replaced by the evaluation with the mean mixture fraction.

Case	1	2	3
Re	7100	12781	7100
Jet exit velocity, $u_0[m/s]$	25	45	25
Coflow velocity, $u_\infty[m/s]$	0.34	0.34	0.74

Table 1: Simulated inflow conditions

NUMERICAL SIMULATION

The presented model is validated using the experimental data for lifted methane/air jet diffusion flames by (Muñiz and Mungal 1997). Lift-off heights have been measured for varying jet axis and coflow velocities. Three different cases have been considered, a baseline case far from blowout, and in addition a variation in both the jet exit velocity and the coflow velocity. The latter two cases are close to the blowoff limit. The inflow conditions for the three cases are given in Table 1.

The simulations have been performed using an axisymmetric low Mach number LES code by Pierce and Moin (1998). In addition to the equations for the cold flow the G-equation and the equation for the mixture fraction are solved. The coefficients of all sub-grid models used in the simulation are determined applying the dynamic model by Moin et al. (1991). The simulation is performed for a domain length of $50\,D$ for case 1 and $60\,D$ for cases 2 and 3 and a diameter of $30\,D$ for all cases, where $D = 0.0048\,\mathrm{m}$ is the diameter of the fuel nozzle. The computational mesh consists of $256 \times 96 \times 64$ grid points resulting in approximately 1.7 million cells. The inflow conditions are generated from a separate LES of a turbulent pipe flow with the appropriate bulk velocity and Reynolds number. The chemical mechanism used to compute both the laminar diffusion flamelets and the laminar burning velocities is GRI 2.11 (Bowman et al. 1995).

RESULTS AND DISCUSSION

Results of the numerical simulations are shown in Fig. 1 and 2. Figure 2 shows instantaneous fields of the density distribution for all three test cases. The black lines indicate stoichiometric mixture fraction and the white lines are the instantaneous flame position. For all cases the stabilization point is far downstream of the nozzle. Since the density in the unburnt region is conserved it gives an additional indication for the development of the mixture fraction field.

It can be observed for all three cases that the stabilization occurs in the lean part of the flame. This is caused by the fact that the local velocities in this part are very low, while the local mixture fraction value might still allow

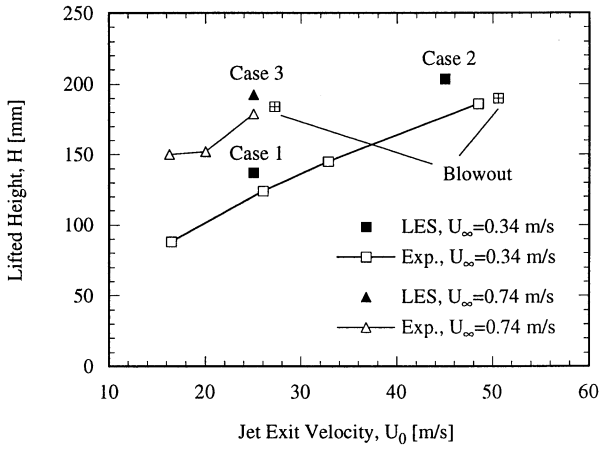

Figure 1: Comparison of computed lift-off heights with experimental data

for flame propagation. It can also be seen that in general the instantaneous flame front cuts the stoichiometric contour almost perpendicularly, while the flames aligns with the mixture fraction for values much lower and much higher than stoichiometric.

As expected, the increase in jet exit velocity increases the lift-off height. Case 2 is already very close to the blowout limit. Due to the higher velocity compared to the coflow velocity the jet spreading rate is higher and hence the unburnt rich cone penetrating into the burning region around the centerline is much wider. Behind the flame front the widening of the jet due to gas expansion can be observed from the stoichiometric mixture fraction contour.

Case 3 has the same jet exit velocity as case 1, but an increased coflow velocity. Although the coflow velocity is almost two orders of magnitude lower than the jet velocity, the influence is very strong as shown in Fig. 2. The increased coflow velocity also results in a reduced spreading rate of the jet. The flame base therefore appears much narrower as for the other cases.

The comparison with the experimental data is shown in Fig. 1. The data are slightly overpredicted, but still in reasonably good agreement. Particularly the trends are predicted very well.

ACKNOWLEDGEMENTS

This work was funded in part by the US Department of Energy within the ASCI program. This support is gratefully acknowledged. The authors are indebted to Charles Pierce for providing his LES computer code.

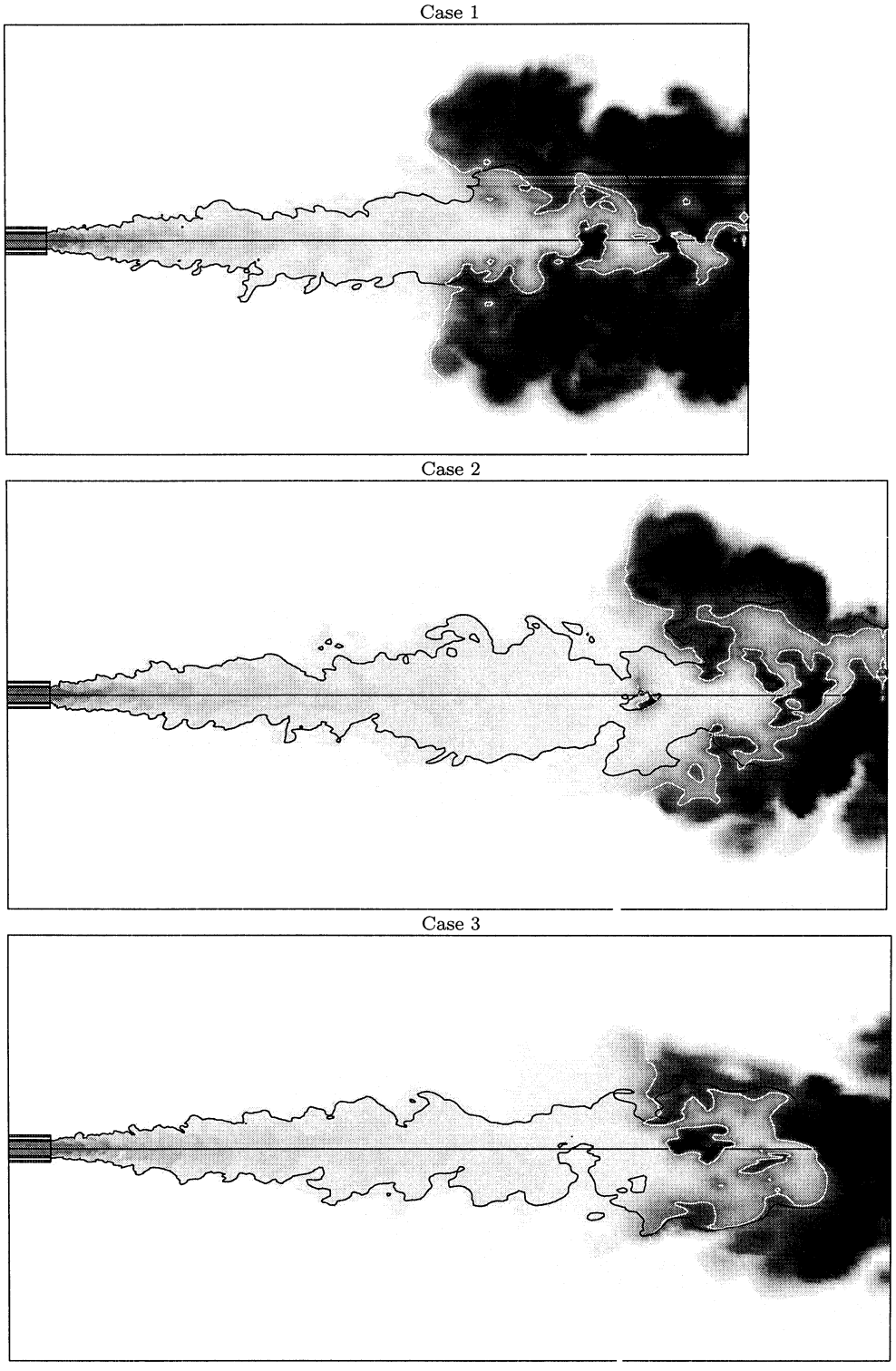

Figure 2: Instantaneous density distribution for case 1, 2, and 3. Black lines are the stoichiometric mixture fraction, white lines indicate the instantaneous flame position ($G = G_0$).

REFERENCES

Bowman, C. T., Hanson, R. K., Davidson, D. F., Gardiner, Jr., W. C., Lissianski, V., Smith, G. P., Golden, D. M., Frenklach, M. and Goldenberg, M. (1995), 'Gri-mech 2.11', http://www.me.berkeley.edu/gri_mech/.

Chen, M., Herrmann, M. and Peters, N. (1999), 'Flamelet modeling of lifted turbulent methane/air and propane/air jet diffusion flames', *Proc. Combust. Inst.* **28**. accepted.

Clavin, P. and Williams, F. A. (1982), 'Effects of molecular diffusion and of thermal expansion on the structure and dynamics of premixed flames in turbulent flows of large scale and low intensity', *J. Fluid Mech.* **116**, 251–282.

Duchamp de Lageneste, L. and Pitsch, H. (2000), 'A level-set approach to large eddy simulation of premixed turbulent combustion', *CTR Annual Research Briefs* pp. 105–116.

Kioni, P. N., Rogg, B., Bray, K. N. C. and Liñán, A. (1993), 'Flame spread in laminar mixing layers: The triple flame', *Comb. Flame* **95**, 276.

Moin, P., Squires, K., Cabot, W. and Lee, S. (1991), 'A dynamic subgrid-scale model for compressible turbulence and scalar transport', *Phys. Fluids A* **3**, 2746–2757.

Muñiz, L. and Mungal, M. G. (1997), 'Instantaneous flame-stabilization velocities in lifted-jet diffusion flames', *Comb. Flame* **111**, 16–31.

Müller, C. M., Breitbach, H. and Peters, N. (1994), 'Partially premixed turbulent flame propagation in jet flames', *Proc. Combust. Inst.* **25**, 1099–1106.

Pelce, P. and Clavin, P. (1982), 'Influence of hydrodynamics and diffusion upon the stability limits of laminar premixed flames', *J. Fluid Mech.* **124**, 219–237.

Peters, N. (1999), 'The turbulent burning velocity for large scale and small scale turbulence', *J. Fluid Mech.* **384**, 107–132.

Peters, N. (2000), *Turbulent Combustion*, Cambridge University Press.

Peters, N. and Williams, F. A. (1983), 'Liftoff characteristics of turbulent jet diffusion flames', *AIAA J.* **21**(3), 423–429.

Pierce, C. D. and Moin, P. (1998), 'A dynamic model for subgrid-scale variance and dissipation rate of a conserved scalar', *Phys. Fluids* **10**, 3041–3044.

Pitsch, H. (2000), 'Unsteady flamelet modeling of differential diffusion in turbulent jet diffusion flames', *Comb. Flame* **123**, 358–374.

Pitsch, H., Chen, M. and Peters, N. (1998), 'Unsteady flamelet modeling of turbulent hydrogen/air diffusion flames', *Proc. Combust. Inst.* **27**, 1057–1064.

Pitsch, H. and Steiner, H. (2000*a*), 'Large-eddy simulation of a turbulent piloted methane/air diffusion flame (Sandia flame D)', *Phys. Fluids* **12**(10), 2541–2554.

Pitsch, H. and Steiner, H. (2000*b*), 'Scalar mixing and dissipation rate in large-eddy simulations of non-premixed turbulent combustion', *Proc. Combust. Inst.* **28**. accepted.

Pitts, W. M. (1988), 'Assessment of theories for the behavior and blowout of lifted trubulent jet diffusion flames', *Proc. Combust. Inst.* **22**, 809–816.

Plessing, T., Terhoeven, P., Mansour, M. S. and Peters, N. (1998), 'An experimental and numerical study of a laminar triple flame', *Comb. Flame* **115**, 335–353.

Ruetsch, G. R., Vervisch, L. and Liñán, A. (1995), 'Effects of heat release on triple flames', *Phys. Fluids* **7**(6), 1447–1454.

Russo, G. and Smereka, P. (2000), 'A remark on computing distance functions', *J. Comp. Phys.* **163**, 51–67.

Vanquickenborne, L. and van Tiggelen, A. (1966), 'The stabilization mechanism of lifted diffusion flames', *Comb. Flame* **10**, 59.

Williams, F. A. (1985*a*), *Combustion Theory*, The Addison-Wesley Publishing Company.

Williams, F. A. (1985*b*), Turbulent combustion, *in* J. D. Buckmaster, ed., 'The Mathematics of Combustion', Society for Industrial & Applied Mathematics, pp. 197–1318.